Available online at www.sciencedirect.com
SCIENCE DIRECT®
Journal of Solid State Chemistry 178 (2005) 2686–2691
JOURNAL OF SOLID STATE CHEMISTRY
www.elsevier.com/locate/jssc

$[H_3N(CH_2)_4NH_3]_2[Al_4(C_2O_4)(H_2PO_4)_2(PO_4)_4]\cdot 4[H_2O]$: A new layered aluminum phosphate-oxalate

Li Peng, Jiyang Li, Jihong Yu*, Guanghua Li, Qianrong Fang, Ruren Xu*

State Key Lab of Inorganic Synthesis and Preparative Chemistry, College of Chemistry, Jilin University, Changchun 130012, PR China

Received 2 February 2005; received in revised form 28 March 2005; accepted 7 April 2005
Available online 18 July 2005

Abstract

A new layered inorganic–organic hybrid aluminum phosphate-oxalate $[H_3N(CH_2)_4NH_3]_2[Al_4(C_2O_4)(H_2PO_4)_2(PO_4)_4]\cdot 4[H_2O]$(AlPO-CJ25) has been synthesized hydrothermally, by using 1,4-diaminobutane (DAB) as structure-directing agent. The structure has been solved by single-crystal X-ray diffraction analysis and further characterized by IR, ^{31}P MAS NMR, TG-DTA as well as compositional analyses. Crystal data: the triclinic space group P-1, $a = 8.0484(7)$ Å, $b = 8.8608(8)$ Å, $c = 13.2224(11)$ Å, $\alpha = 80.830(6)^\circ$, $\beta = 74.965(5)^\circ$, $\gamma = 78.782(6)^\circ$, $Z = 2$, $R_{1[I>2\sigma(I)]} = 0.0511$ and $wR_{2(\text{all data})} = 0.1423$. The alternation of AlO_4 tetrahedra and PO_4 tetrahedra gives rise to the four-membered corner-sharing chains, which are interconnected through AlO_6 octahedra to form the layered structure with 4,6-net sheet. Interestingly, oxalate ions are bis-bidentately bonded by participating in the coordination of AlO_6, and bridging the adjacent AlO_6 octahedra. The layers are held with each other through strong H-bondings between the terminal oxygens. The organic ammonium cations and water molecules are located in the large cavities between the interlayer regions.

Keywords: Layer; Aluminum phosphate-oxalate; Synthesis; Structure

1. Introduction

Following the discovery of microporous aluminophosphates $AlPO_4$-n (n denotes a specific structure type) [1], there is considerable interest in developing new aluminophosphate compounds with novel framework structures due to their potential applications in catalysis, adsorption, and separation [2–4]. Recently, a large number of aluminophosphates with 2D layered structures have been prepared by the employment of organic amines as the structure-directing agents (SDAs) under hydrothermal/ solvothermal conditions [5]. These compounds consist of anionic aluminophosphate sheets, normally held together by positively charged organic molecules through H-bondings. The anionic sheets made up of alternation of Al-centered polyhedra (AlO_4, AlO_5, AlO_6) and P-centered tetrahedra $P(O_b)_n(O_t)_{4-n}$ (b, bridging; t, terminal; $n = 2, 3, 4$) show a great variety of compositions and architectures. Introduction of species which possess a bridging functionality, such as the oxalate ions, may offer a further opportunity in the creation of novel structural features in the AlPOs chemistry. As a matter of fact, a large number of phosphate-oxalates of V [6–9], Mn [10,11], Fe [12–19], Ga [20–25], In [26], Sn [27,28], Co [29], Zn [30] and mixed-metal phosphate-oxalates [31] have been reported during the past few years. In most cases, these materials have 3D structures built up of metal phosphate layers connected by oxalate ligands. The incorporation of oxalate units within the inorganic layers has been observed only in a few examples [9,19–21,26,29,31].

In the case of aluminophosphate, three aluminum phosphate-oxalates with novel 2D [32] and 3D [33,34] structural features have been obtained. The oxalate

---

*Corresponding author. Fax: +86 431 5168608.
E-mail addresses: jihong@mail.jlu.edu.cn (J. Yu), rrxu@mail.jlu.edu.cn (R. Xu).

0022-4596/$ - see front matter © 2005 Elsevier Inc. All rights reserved.
doi:10.1016/j.jssc.2005.04.039

units participate in the coordination of Al atoms, and exhibit bidentate and bis-bidentate coordination mode in the 2D structure and 3D structure, respectively.

Here we report the synthesis and structure of a new 2D layered aluminum phosphate-oxalate AlPO-CJ25 templated by 1,4-diaminobutane (DAB). It is not only the first example of 2D aluminum phosphate-oxalate that contains bis-bidentate coordination mode of oxalate within the metal phosphate layer but also the first example of layered aluminophosphate that contains one-bridged PO_4 treahedra.

2. Experimental section

AlPO-CJ25 was synthesized by a hydrothermal reaction of the mixture of aluminum isopropoxide ((*i*-PrO)$_3$Al), H_3PO_4, oxalic acid dihydrate (ox), 1,4-diaminobutane (DAB) and water in the molar ratio 1:2:4:3:227. In a typical synthesis, 0.5g (*i*-PrO)$_3$Al was first dissolved in 10 mL of water and then 0.33 mL of phosphoric acid (85 wt%) and 1.2 g ox were added with stirring. Finally, 0.7 mL of DAB was added to the above reaction mixture. The resulting solution was stirred for 1 h until it was homogeneous, and then was sealed in a Teflon-lined stainless steel autoclave and heated at 180 °C for 24 h under static conditions. Colorless plate-like crystals were separated from the mother liquor by filtration and further washed by distilled water and then air-dried. The yield is 55% based on Al.

Inductively coupled plasma (ICP) analysis was performed on a Perkin–Elmer Optima 3300 DV ICP instrument, which gave the contents of Al as 10.43 wt% and P as 18.18 wt% (calc. Al 10.56; P18.20). Elemental analyses conducted on a Perkin–Elmer 2400 elemental analyzer gave the contents of C as 11.67 wt%, H as 3.98 wt%, and N as 5.51 wt% (calc. C 11.74, H 3.91, N 5.48).

The infrared (IR) spectrum of the products was recorded on a BRUKER VECTOR22 Spectrometer with the KBr-disk technique.

A Perkin–Elmer TGA 7 unit was used to carry out the thermogravimetric analysis (TGA) in air with a heating rate of 10 °C /min.

A suitable single crystal with dimensions 0.35 × 0.27 × 0.24 mm was selected for single-crystal X-ray diffraction analysis. The intensive data were collected on a Siemens SMART CCD diffractometer using graphite-monochromated MoKα radiation ($\lambda = 0.71073$ Å) at a temperature of 20 ± 2 °C. Data processing was accomplished with the SAINT processing program [35]. The structure was solved in the space group *P*-1 by direct methods and refined by a full-matrix least-squares approach on F^2 by SHELXTL software package [36]. Hydrogen atoms were geometrically placed. All non-hydrogen atoms were anisotropically refined. Experi-

Table 1
Crystal data and structure refinement for AlPO-CJ25

Empirical formula	$C_5H_{20}Al_2N_2O_{16}P_3$
Formula weight	511.10
Temperature	293(2) K
Wavelength	0.71073 Å
Crystal system, space group	Triclinic, *P*-1
Unit cell dimensions	$a = 8.0484(7)$ Å $\alpha = 80.830(6)$ °
	$b = 8.8608(8)$ Å $\beta = 74.965(5)$ °
	$c = 13.2224(11)$ Å $\gamma = 78.782(6)$ °
Volume	887.36(13) Å^3
Z, Calculated density	2, 1.913 Mg/m^3
Absorption coefficient	0.522 mm^{-1}
F(0 0 0)	526
Crystal size	0.35 × 0.27 × 0.24 mm
Theta range for data collection	1.61–28.46 °
Limiting indices	$-10 \leqslant h \leqslant 8$, $-11 \leqslant k \leqslant 8$, $-17 \leqslant l \leqslant 15$
Reflections collected/unique	6412/4380 [*R*(int) = 0.0409]
Completeness to theta = 28.09	97.7%
Refinement method	Full-matrix least-squares on F^2
Data/restraints/parameters	4380/0/266
Goodness-of-fit on F^2	1.066
Final *R* indices [$I > 2\sigma(I)$]	$R_1 = 0.0511$, w$R_2 = 0.1314$
R indices (all data)	$R_1 = 0.0796$, w$R_2 = 0.1423$
Largest diff. peak and hole	0.663 and −0.533 eÅ^{-3}

Table 2
Atomic coordinates ($\times 10^4$) and equivalent isotropic displacement parameters (Å$^2 \times 10^3$) for AlPO-CJ25

	x	*y*	*z*	*U*(eq)
Al(1)	2019(1)	9075(1)	1086(1)	13(1)
Al(2)	2538(1)	14831(1)	−386(1)	13(1)
P(1)	378(1)	12337(1)	29(1)	12(1)
P(2)	902(1)	8697(1)	3656(1)	19(1)
P(3)	6371(1)	14529(1)	−1562(1)	13(1)
O(1)	876(3)	11102(3)	881(2)	17(1)
O(2)	871(3)	9058(3)	2503(2)	18(1)
O(3)	3448(3)	9295(3)	−408(2)	17(1)
O(4)	3405(3)	7197(3)	1276(2)	20(1)
O(5)	333(3)	8268(3)	746(2)	19(1)
O(6)	3974(3)	10010(3)	1325(2)	16(1)
O(7)	1983(3)	13096(3)	−573(2)	17(1)
O(8)	4422(3)	15187(3)	−1314(2)	19(1)
O(9)	955(3)	16395(3)	−612(2)	18(1)
O(10)	2766(4)	14688(3)	907(2)	21(1)
O(11)	1635(5)	6991(4)	3936(2)	50(1)
O(12)	−1059(4)	8958(3)	4279(2)	28(1)
O(13)	1877(4)	9718(4)	4011(2)	29(1)
O(14)	7149(4)	15009(3)	−2717(2)	21(1)
O(1W)	2746(5)	9319(5)	−2456(3)	46(1)
O(2W)	5197(6)	7457(5)	−3851(3)	64(1)
N(1)	−4530(5)	18326(5)	3966(3)	39(1)
N(2)	925(5)	12541(4)	2725(3)	32(1)
C(1)	−3768(8)	17054(7)	3292(4)	54(2)
C(2)	−2674(7)	15758(6)	3816(4)	38(1)
C(3)	−1525(6)	14681(5)	3013(3)	34(1)
C(4)	−495(7)	13311(5)	3521(3)	36(1)
C(5)	4851(5)	9795(4)	−507(3)	15(1)

U(eq) is defined as one third of the trace of the orthogonalized U_{ij} tensor.

Table 3
Selected bond lengths (Å) and angles (°) for AlPO-CJ25

Al(1)–O(1)	1.864(3)	O(4)–Al(1)–O(2)	94.29(12)
Al(1)–O(5)	1.831(3)	O(5)–Al(1)–O(1)	92.58(12)
Al(1)–O(2)	1.860(3)	O(4)–Al(1)–O(1)	172.29(13)
Al(1)–O(4)	1.835(3)	O(2)–Al(1)–O(1)	87.54(11)
Al(1)–O(3)	2.013(3)	O(5)–Al(1)–O(3)	93.87(12)
Al(1)–O(6)	2.026(3)	O(4)–Al(1)–O(3)	87.40(12)
Al(2)–O(10)	1.748(3)	O(2)–Al(1)–O(3)	172.48(10)
Al(2)–O(8)	1.732(3)	O(1)–Al(1)–O(3)	89.82(11)
Al(2)–O(9)	1.736(3)	O(5)–Al(1)–O(6)	174.92(12)
Al(2)–O(7)	1.753(3)	O(4)–Al(1)–O(6)	85.86(12)
P(1)–O(1)	1.516(2)	O(2)–Al(1)–O(6)	91.43(11)
P(1)–O(5)#1	1.503(3)	O(1)–Al(1)–O(6)	86.61(11)
P(1)–O(9)#2	1.545(3)	O(3)–Al(1)–O(6)	81.12(11)
P(1)–O(7)	1.546(3)	P(1)–O(1)–Al(1)	142.11(17)
P(2)–O(13)	1.503(3)	P(2)–O(2)–Al(1)	150.23(18)
P(2)–O(2)	1.512(3)	C(5)–O(3)–Al(1)	113.8(2)
P(2)–O(11)	1.536(3)	P(3)#3–O(4)–Al(1)	150.97(19)
P(2)–O(12)	1.571(3)	P(1)#1–O(5)–Al(1)	151.69(18)
P(3)–O(4)#3	1.502(3)	C(5)#3–O(6)–Al(1)	113.2(2)
P(3)–O(14)	1.519(3)	P(1)–O(7)–Al(2)	128.40(16)
P(3)–O(10)#4	1.550(3)	P(3)–O(8)–Al(2)	138.58(16)
P(3)–O(8)	1.532(3)	P(1)#2–O(9)–Al(2)	140.53(17)
O(5)–Al(1)–O(4)	94.78(13)	P(3)#4–O(10)–Al(2)	139.07(18)
O(5)–Al(1)–O(2)	93.54(12)		

Symmetry transformations used to generate equivalent atoms: #1 $-x, -y+2, -z$, #2 $-x, -y+3, -z$, #3 $-x+1, -y+2, -z$, #4 $-x+1, -y+3, -z$.

mental details for the structure determination are presented in Table 1. Final atomic parameters and the selected bond distances and bond angles are presented in Tables 2 and 3, respectively.

Solid-state ^{31}P MAS NMR spectroscopy was conducted on a Varian Infinity Plus 400 NMR spectrometer operated at 161.90 MHz. The spinning speed was 5 kHz. Chemical shifts were referenced to 85% H_3PO_4. The ^{1}H- ^{31}P CP MAS NMR spectrum was recorded using 2.0 μs ^{1}H (90°) pulse length with a contact time $t_c = 1.0$ ms.

3. Results and discussion

The FTIR spectrum (Fig. 1) displays bands characteristic of oxalate vibrations [$va(C{=}O){\sim}1690\,\mathrm{cm}^{-1}$] and protonated amine [$\delta d(NH^{3+}){\sim}1530\,\mathrm{cm}^{-1}$], thus showing the presence of an organic component.

The results of TG and DTA analyses are given in Fig. 2. The TG curve consists of two distinct parts which are accompanied by two endothermic effects on the DTA curve. The first one with a weight loss of 6.6%, is nearly completed at ca. 300 °C. The second one occurs at 300–800 °C with 24.4% weight loss. The first thermal event corresponds to desorption of water molecule (calc. 7.0%), while the last one can be attributed to a decarbonylation process and the decomposition of DAB species (calc. 25.0%).

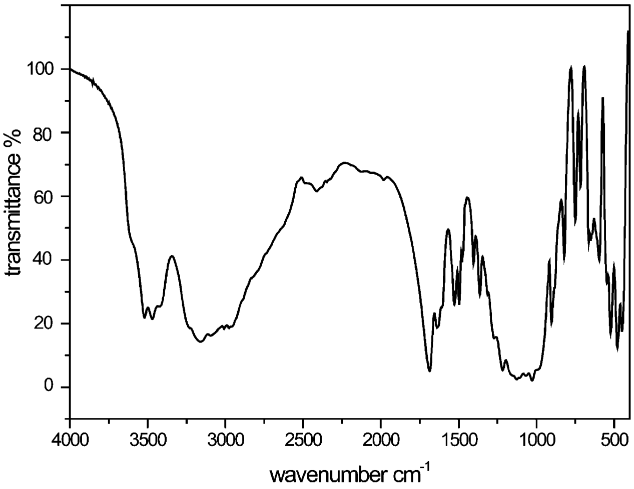

Fig. 1. FTIR spectrum of AlPO-CJ25.

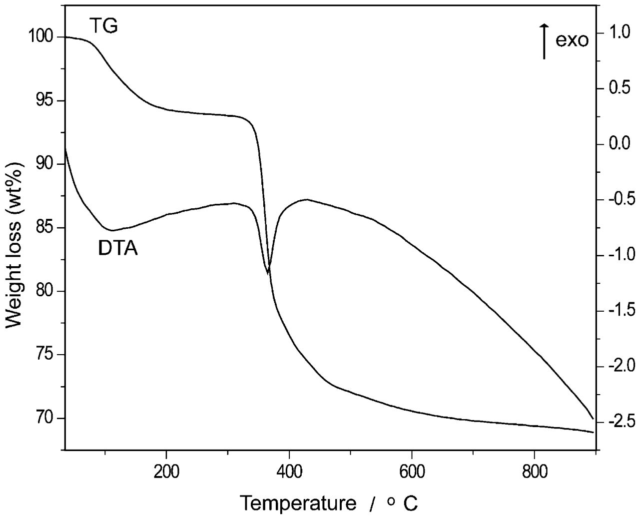

Fig. 2. TG-DTA curves.

Single-crystal structural analysis shows that AlPO-CJ25 has the empirical formula $[H_3N(CH_2)_4NH_3]_2[Al_4(C_2O_4)(H_2PO_4)_2(PO_4)_4]\cdot 4[H_2O]$. It crystallizes in the triclinic space group *P*-1 with the lattice parameters $a = 8.0484(7)$ Å, $b = 8.8608(8)$ Å, $c = 13.2224(11)$ Å, $\alpha = 80.830(6)°$, $\beta = 74.965(5)°$, $\gamma = 78.782(6)°$. The asymmetric unit, as seen in Fig. 3, contains two crystallographically distinct Al atoms and three P atoms. Al(1) is octahedrally coordinated and shares four oxygens with P atoms, while the remaining two vertexes belong to an oxalate group. The coordination by the oxalate leads to a distorted octahedron for Al(1), as indicated by the wide range of Al(1)–O bond lengths [1.831(3)–2.026(3) Å] and the O–Al–O bond angle [81.12(11)°] subtended by the oxalate group. Al(2) is tetrahedrally coordinated and shares four oxygens with the adjacent P atoms. The Al(2)–O bond lengths are in

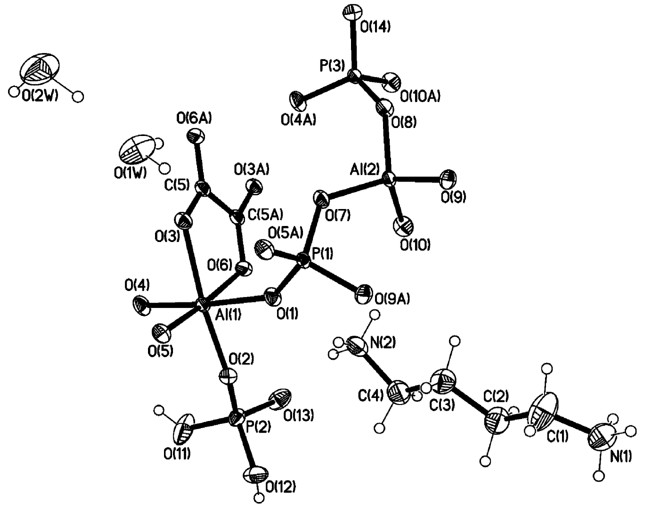

Fig. 3. Thermal ellipsoid plot (50% probability) and atomic labeling scheme of AlPO-CJ25.

the range of 1.732(3)–1.753(3) Å. The three crystallographically distinct P atoms are tetrahedrally coordinated. P(1) has four oxygen atoms bridging to the adjacent Al atoms, and the P(1)–O bond lengths vary within the range of 1.503(3)–1.546(3) Å. P(2) shares only one oxygen with the adjacent Al atom with the P–O bond length of 1.512(3) Å, and the remaining vertices are one shorter P–O bond (P(2)–O(13): 1.503(3) Å) and two longer P–O bonds (P(2)–O(11): 1.536(3) Å, P(2)–O(12): 1.571(3) Å). P(3) shares three oxygens with adjacent Al atoms (P–O bond lengths: 1.502(3)–1.550(3) Å) and remains one P–O bond (P(3)–O(14): 1.519(3) Å). Bond-valence calculations indicate that O(11), O(12), O(13) and O(14) have valence sums of 1.25, 1.14, 1.37 and 1.31, respectively, and all other oxygen atoms have values close to 2 [37]. The valence sums of O(13) and O(14) can be satisfied by forming hydrogen bonds with hydrogen phosphate groups, 1,4-diaminobutane cations, and waters [O(13)…O(12) = 2.59 Å, O(13)…N(1) = 2.90 Å, O(13)…N(2) = 2.89 Å, O(14)…O(11) = 2.47 Å, O(14)…O(2W) = 2.88 Å, O(14)…N(2) = 2.90 Å]. To balance charge, all other O atoms with undersaturated valence sums are hydroxo oxygens. Therefore, P(1) is PO_4 group, P(2) is H_2PO_4 group, and P(3) is $PO_3(=O)$ group.

The present of three types of monophosphates in the structure is confirmed by ^{31}P MAS NMR spectrum (Fig. 4a) which shows three peaks at −7.85, −18.01 and −22.92 ppm with relative intensities close to 1:1:1. On the basis of the previous studies [38], it clearly indicated that the peak at −7.85 ppm to P(2) (H_2PO_4 group), peak at −18.01 ppm to P(3) ($PO_3(=O)$ group), and −22.92 ppm to P(1) (PO_4 group). The $^1H \rightarrow {}^{31}P$ CP MAS NMR spectrum is shown in Fig. 4b. The most prominent difference between the $^1H \rightarrow {}^{31}P$ CP MAS NMR spectrum and the ^{31}P MAS NMR spectrum is that in the first spectrum the resonance at −7.85 ppm is greatly enhanced. Poor CP efficiencies for the resonances at −18.01 and −22.92 ppm indicate that these P atoms are not proximity to the protons, consistent with the assignment of these resonances to the $PO_3(=O)$ and PO_4 groups. Therefore, there is a good correlation between the NMR spectrum and the structure.

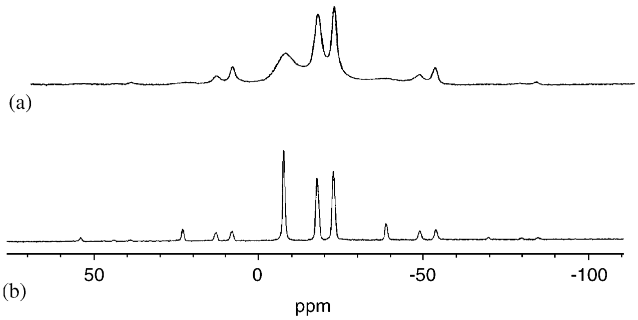

Fig. 4. ^{31}P MAS NMR (a) and $^1H \rightarrow {}^{31}P$ CP MAS NMR (b) spectra of AlPO-CJ25.

The macroanionic inorganic–organic hybrid layer is a new type of 4,6 net sheet as seen in Fig. 5. There are two basic building units in this sheet, i.e., 1D aluminophosphate chain built up by corner-sharing Al_2P_2 4-MRs, denoted as AlPO-CSC chain, and dimer of oxalate-bridged two AlO_6 octahedra with pendant H_2PO_4 group, denoted as D-AlO_6. This type of AlPO-CSC chain is a fundamental chain [39–41] that can be found in a range of aluminophosphate frameworks. The AlPO-CSC chains parallel to the [100] direction are linked to each other by sharing oxygens with AlO_6 octahedra. Oxalate anions act as bis-bidentate ligands to octahedral Al atoms, and form dimers of AlO_6 octahedra. The pendant H_2PO_4 groups, perpendicular to the layers, connected to the octahedral Al atoms by oxygens. This kind of $P(O_b)(O_t)_3$ (b, bridging; t, terminal) tetrahedron can be found in two 1D chains [42,43], but it is the first time to be found in the 2D layered structures of aluminophosphates.

As seen in Fig. 6, the sheets stack in an AAAA sequence along the [001] direction, and are held together through strong H-bondings between the terminal O atoms attached to P(2) tetrahedra protruding into the interlayer region. The O…O distance between O(12) and O(13) from the adjacent layer is 2.587(4) Å and an O(12)-H…O(13) angle is 124.3 °. Strong H-bondings are also found to exist between O(11) and O(14) within the layer, with the O(11)…H–O(14) separation of 2.472(4) Å and the O(11)…H–O(14) angle of 153.8°. Large cavities are formed between the two layers, in which diprotonated DAB and water molecules reside. The anionic framework is further stabilized by forming multi-hydrogen-bonding with water and the organic cations. Table 4 summarizes the H-bond information.

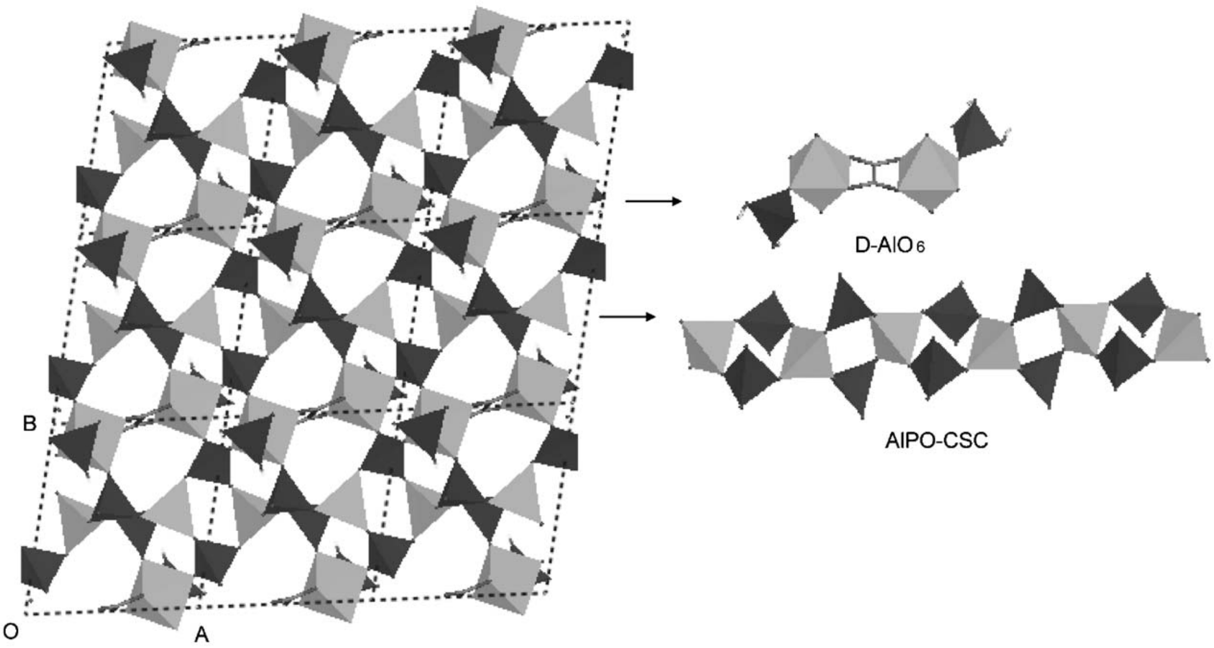

Fig. 5. Polyhedral representations of layer and substructures in AlPO-CJ25. Left: The organic–inorganic sheet parallel to the *ab* plane; right: 1D corner-sharing aluminophosphate chain (AlPO-CSC chain) and Dimer of oxalate-bridged two AlO_6 octahedra with pendant H_2PO_4 group (D-AlO_6).

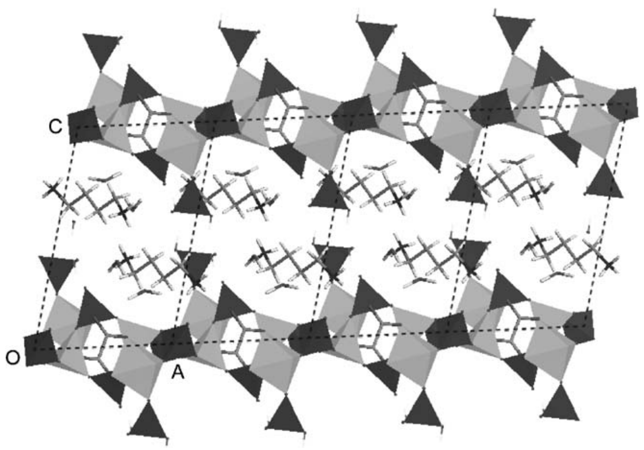

Fig. 6. Packing of the sheets in an AAAA sequence along the [100] direction.

Table 4
H-Bonds for AlPO-CJ25

D-H…A	*d*(D-H)	*d*(H…A)	*d*(D…A)	<(DHA)
O(11)–H(11)…O(14)♯3	0.82	1.71	2.472(4)	153.8
O(12)–H(12)…O(13)♯5	0.82	2.04	2.587(4)	124.3
O(1W)–H(1WA)…O(3)	1.09(7)	2.21(6)	2.903(4)	119(4)
O(1W)–H(1WB)…O(2)♯1	0.99(7)	2.06(7)	2.997(5)	156(5)
O(2W)–H(2WA)…O(1W)	1.01(6)	1.82(6)	2.798(6)	162(5)
O(2W)–H(2WB)…O(14)♯6	1.01(7)	1.91(7)	2.878(5)	160(6)
N(1)–H(1A)…O(13)♯7	0.89	2.27	2.904(5)	127.8
N(1)–H(1B)…O(12)♯8	0.89	2.24	3.094(5)	161.9
N(1)–H(1C)…O(2W)♯9	0.89	2.16	2.829(6)	131.7
N(2)–H(2A)…O(13)	0.89	2.04	2.882(5)	157.0
N(2)–H(2B)…O(14)♯4	0.89	2.16	2.900(5)	139.7
N(2)–H(2B)…O(10)	0.89	2.26	3.064(4)	150.2
N(2)–H(2C)…O(1)	0.89	2.14	2.938(5)	148.9

Symmetry transformations used to generate equivalent atoms: ♯1 $-x,-y+2,-z$, ♯3 $-x+1,-y+2,-z$, ♯4 $-x+1,-y+3,-z$, ♯5 $-x,-y+2,-z+1$, ♯6 $x,y-1,z$, ♯7 $x-1,y+1$, z, ♯8 $x,y+1,z$, ♯9 $x-1,y+1,z+1$.

AlPO-CJ25 is characterized by the presence of oxalate which acts as a bis-bidentate ligand within the layers. Due to all of the oxygen atoms belong to the oxalate have been connected with the Al atoms within the sheets, this compound cannot expand to 3D structure as other common metal phosphate-oxalates in which oxalates connect layers by participating in the coordination of metal atoms belong to the adjacent sheets. To the best of our knowledge, this is one of few examples [20,31] where such a coordination mode is observed. For most layered metal phosphate-oxalates, the oxalate group acts as a bidentate ligand to the MeO_6 octahedron in a direction perpendicular to the plane of the layers. It will be instructive to summery the coordination mode of oxalate that can be found in the others aluminum phosphate-oxalates. In the layered aluminum phosphate-oxalate obtained in the presence of 1,2-diaminoethane [32], oxalate unit exhibits bidentate coordination mode, which chelates one aluminum atom and has two terminal C–O groups pendent to the layers as most layered metal phosphate-oxalates. In both aluminum phosphate-oxalates with 3D structures, the oxalate units are bonded similarly—in the bis-bidentate manner. For the aluminum phosphate-oxalate with gmelinite-like structure [33], the entire framework is built form the double six-rings linking to each other via oxalate. While for the aluminum phosphate-oxalate prepared by 1,2-diaminopropane [34], its structure has features common to other metal phosphate-oxalates, and is built of metal phosphate layers pillared by oxalate to form a 3D framework. This clearly shows that oxalate units with a bonding flexibility, can significantly expand structure specificity and diversity of aluminophosphates.

4. Conclusions

The hydrothermal synthesis of a new layered aluminum phosphate-oxalate $[H_3N(CH_2)_4NH_3]_2[Al_4(C_2O_4)(H_2PO_4)_2(PO_4)_4]\cdot4[H_2O]$ and its structural characterization have been described in this work. The compound presents two new structure feathers for the layered aluminophosphates: one is the incorporation of bis-bidentate oxalate units within the inorganic layers, and the other one is the $P(Ob)_1(Ot)_3$ tetrahedron. The novel connection mode showed by this compound illustrates that incorporation of organic ligands can dramtically manipulate the structure, and it is a useful method for the design of new materials with novel structure.

Acknowledgments

We are grateful to the National Natural Science Foundation of China and the State Basic Research Project (G2000077507) for financial supports.

References

[1] S.T. Wilson, B.M. Lok, C.A. Messian, T.R. Cannan, E.M. Flanigen, J. Am. Chem. Soc. 104 (1982) 1146.
[2] W.H. Meier, D.H. Olson, C. Baerlocher, Atlas of Zeolite Structure Types, Elsevier, London, 2001.
[3] J.M. Bennett, W.J. Dytrych, J.J. Pluth, J.W. Richardson Jr., J.V. Smith, Zeolites 6 (1986) 349.
[4] J.M. Thomas, R. Raja, G. Sankar, R.G. Bell, Acc. Chem. Res. 34 (2001) 191.
[5] J. Yu, R. Xu, Acc. Chem. Res. 36 (2003) 481, and references therein.
[6] Y.-M. Tsai, S.-L. Wang, C.-H. Huang, K.-H. Lii, Inorg. Chem. 38 (1999) 4183.
[7] J. Do, R.P. Bontchev, A.J. Jacobson, Inorg. Chem. 39 (2000) 3230.
[8] J. Do, R.P. Bontchev, A.J. Jacobson, Chem. Mater. 13 (2001) 2601.
[9] M.-F. Tang, K.-H. Lii, J. Solid State Chem. 177 (2004) 1912.
[10] Z.A.D. Lethbridge, S.K. Tiwary, A. Harrison, P. Lightfoot, J. Chem. Soc. Dalton Trans. (2001) 1904.
[11] Z.A.D. Lethbridge, A.D. Hillier, R. Cywinski, P. Lightfoot, J. Chem. Soc. Dalton Trans. (2000) 1595.
[12] H.-M. Lin, K.-H. Lii, Y.-C. Jiang, S.-L. Wang, Chem. Mater. 11 (1999) 519.
[13] W.-J. Chang, H.-M. Lin, K.-H. Lii, J. Solid State Chem. 157 (2001) 233.
[14] Z.A.D. Lethbridge, P. Lightfoot, J. Solid State Chem. 143 (1999) 58.
[15] A. Choudhury, S. Natarajan, C.N.R. Rao, J. Solid State Chem. 146 (1999) 538.
[16] A. Choudhury, S. Natarajan, C.N.R. Rao, Chem. Mater. 11 (1999) 2316.
[17] A. Choudhury, S. Natarajan, J. Mater. Chem. 9 (1999) 3113.
[18] Y.-C. Jiang, S.-L. Wang, K.-H. Lii, Chem. Mater. 15 (2003) 1633.
[19] A. Choudhury, S. Natarajan, C.N.R. Rao, Chem. Eur. J. 6 (2000) 1168.
[20] K.-H. Lii, C.-Y. Chen, Inorg. Chem. 39 (2000) 3374.
[21] M. Mrak, U. Kolitsch, C. Lengauer, V. Kaučič, E. Tillmanns, Inorg. Chem. 42 (2003) 598.
[22] C.-Y. Chen, P.-P. Chu, K.-H. Lii, Chem. Commun. (1999) 1437.
[23] L.-C. Hung, H.-M. Kao, K.-H. Lii, Chem. Mater. 12 (2000) 2411.
[24] C.T.S. Choi, E.V. Anokhina, C.S. Day, Y. Zhao, F. Taulelle, C. Huguenard, Z. Gan, A. Lachgar, Chem. Mater. 14 (2002) 4096.
[25] T. Loiseau, G. Férey, M. Haouas, F. Taulelle, Chem. Mater. 16 (2004) 5318.
[26] Y.-F. Huang, K.-H. Lii, J. Chem. Soc. Dalton Trans. (1998) 4085.
[27] S. Natarajan, J. Solid State Chem. 139 (1998) 200.
[28] B. Adair, S. Natarajan, A.K. Cheetham, J. Mater. Chem. 8 (1998) 1477.
[29] A. Choudhury, S. Natarajan, Solid State Sci. 2 (2000) 365.
[30] S. Neeraj, S. Natarajan, C.N.R. Rao, J. Chem. Soc. Dalton Trans. (2001) 289.
[31] W.-M. Chang, S.-L. Wang, Chem. Mater. 17 (2005) 74.
[32] P. Lightfoot, Z.A.D. Lethbridge, R.E. Morris, D.S. Wragg, P.A. Wright, J. Solid State Chem. 143 (1999) 74.
[33] K. Kedarnath, A. Choudhury, S. Natarajan, J. Solid State Chem. 150 (2000) 324.
[34] N. Rajic, N.Z. Logar, G. Mali, V. Kaucic, Chem. Mater. 15 (2003) 1734.
[35] SMART and SAINT software packages, Siemens Analytical X-ray Instruments, Inc., Madison, WI, 1996.
[36] G.M. Sheldrick, SHELXL Program, Version 5.1, Siemens Industrial Automation, Inc., Madison, WI, 1997.
[37] I.D. Brown, D. Altermann, Acta Crystallogr. B 41 (1985) 244.
[38] H. Nakayama, T. Eguchi, N. Nakamura, S. Yamaguchi, M. Danjyo, M. Tsuhako, J. Mater. Chem. 7 (1997) 1063.
[39] Q. Huo, R. Xu, S. Li, Z. Ma, J.M. Thomas, R.H. Jones, A.M. Chippindale, J. Chem. Soc. Chem. Commun. (1992) 875.
[40] A.M. Chippindale, A.V. Powell, L.M. Bull, R.H. Jones, A.K. Cheetham, J.M. Thomas, R. Xu, J. Solid State Chem. 96 (1992) 199.
[41] B. Wei, J. Yu, Z. Shi, S. Qiu, W. Yan, O. Terasaki, Chem. Mater. 12 (2000) 2065.
[42] S. Oliver, A. Kuperman, A. Lough, G.A. Ozin, Chem. Mater. 8 (1996) 2391.
[43] I.D. Williams, J. Yu, Q. Gao, J. Chen, R. Xu, Chem. Commun. (1997) 1273.